The EMBO Journal Vol. 22 No. 6 pp. 1389–1397, 2003

High-resolution sperm typing of meiotic recombination in the mouse MHC E_β gene

C.L.Yauk[1,2], P.R.J.Bois[3] and A.J.Jeffreys

Department of Genetics, University of Leicester, Leicester, LE1 7RH, UK

[1]Present address: Environmental Health Centre, Health Canada, Tunney's Pasture, Ottawa, Ontario, Canada K1A 0L2
[3]Present address: St Jude Children's Research Hospital, Department of Genetics, 332 N. Lauderdale, Memphis, TN 38105, USA

[2]Corresponding author
e-mail: Carole_Yauk@hc-sc.gc.ca

Meiotic crossovers detected by pedigree analysis in the mouse MHC cluster into hotspots. To explore the properties of hotspots, we subjected the class II E_β gene to high-resolution sperm crossover analysis. We confirm the presence of a highly localized hotspot 1.0–1.6 kb wide in the second intron of E_β and show that it is flanked by DNA which is almost completely recombinationally inert. Mice heterozygous for haplotype *s* and another MHC haplotype show major haplotype-dependant variation in crossover rate but always the same hotspot, even in crosses including the highly diverged *p* haplotype. Crossovers in reciprocal orientations occur at similar rates but show different distributions across the hotspot, with the position of centre points in the two orientations shifted on average by 400 bp. This asymmetry results in crossover products showing biased gene conversion in favour of hotspot markers from the non-initiating haplotype, and supports the double-strand break repair model of recombination, with haplotype *s* as the most efficient crossover initiator. The detailed behaviour of the E_β hotspot, including evidence for highly localized recombination initiation, is strikingly similar to human hotspots.

Keywords: gene conversion/meiotic drive/meiotic recombination hotspot/mouse MHC E_β gene

Introduction

There is growing evidence that meiotic crossovers are not distributed randomly along mammalian chromosomes. Rather, mammalian genomes appear, at least to some extent, to be a mosaic of recombinationally suppressed regions separated by intervals that undergo very elevated and targeted crossover activity (Pittman and Schimenti, 1998; Petes, 2001; Yu *et al*., 2001). Recently, high-resolution sperm typing has shown that crossovers in the human MHC tend to cluster into very narrow (1–2 kb) recombination hotspots separated by long stretches of DNA exhibiting strong linkage disequilibrium (Jeffreys *et al*., 2000, 2001). Similarly, meiotic recombination events in the mouse MHC also show strong clustering. Eight mouse hotspots have been identified so far by breakpoint mapping in recombinant inbred lines and in pedigrees. These hotspots vary in the degree to which they have been characterized, from the E_α-*C4* region at 300 kb in length (Lafuse *et al*., 1989), down to the E_α hotspot ~0.5 kb wide (Khambata *et al*., 1996).

Mouse studies have also shown that hotspot location and/or intensity can be influenced by MHC haplotype, as well as genetic background (strain of mouse) and sex (Steinmetz *et al*., 1987; Shiroishi *et al*., 1991, 1993, 1995). For example, the very active hotspot in the class II E_β gene, first characterized by Steinmetz *et al*. (1982), is ~4 kb wide. Its activity varies between hybrid strains, and appears to be completely suppressed in heterozygotes carrying the *p* haplotype, in which crossovers occur instead preferentially at the $E\alpha$ gene (Lafuse and David, 1986; Zimmerer and Passmore, 1991). Heine *et al*. (1994) found that these E_α haplotype *p* recombinants only result when *p* is from the intra-H2 recombinant strain B10F(13R), suggesting that distal modifiers of crossover can influence hotspot activity. Similarly, crossover rates at the *Psmb9* (formerly known as *Lmp*2) hotspot are governed not only by haplotype and genetic background, but also by the sex of the animal, with high female rates occurring only in some strains (Shiroishi *et al*., 1993, 1995).

While crossover breakpoint mapping in mice has provided valuable information about meiotic recombination, the use of recombinant inbred lines and backcrossed offspring to identify MHC-recombinant progeny is extremely laborious. The limited numbers of crossovers that can be detected prevent the detailed definition of hotspot morphology and of the recombination processes operating within hotspots. Similarly, little is known about the recombinational activity of DNA outside these mouse hotspots. These limitations can be overcome by recovering crossover products directly from sperm DNA (Jeffreys *et al*., 1998, 2001), as shown by Guillon and De Massy (2002), who mapped 69 sperm recombinants at the *Psmb9* locus to show that crossover density was maximal in an interval of 210 bp and decreased roughly symmetrically on both sides, in a manner similar to human recombination hotspots. We now extend this approach to analyse recombination at the mouse E_β locus and to investigate the influence of haplotype on male recombination rates and on the distribution and reciprocity of crossover events within the hotspot. We show that the E_β hotspot shares remarkably similar properties with its counterparts in the human MHC, implying similar recombination processes in these two very different species.

Results

Detection of meiotic crossovers in sperm DNA

Re-sequencing across the E_β gene did not reveal any previously unidentified polymorphisms across the crossover hotspot region in the second intron (see Materials and

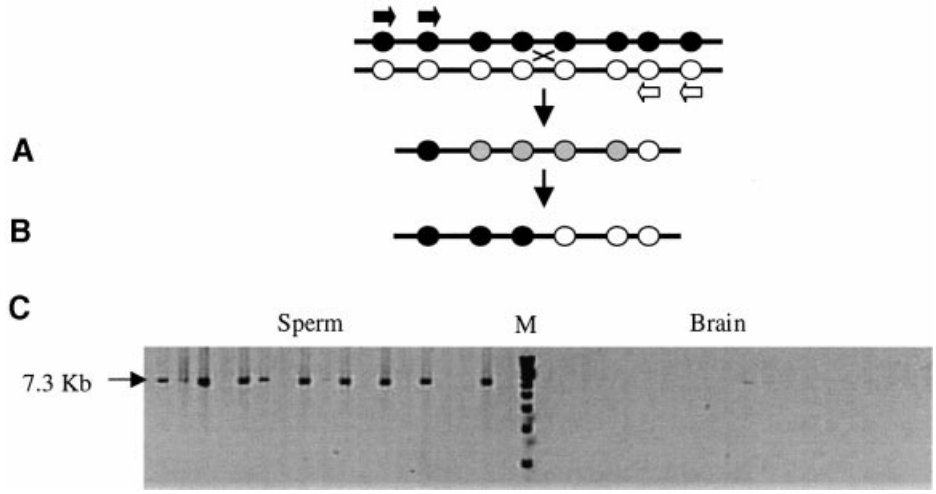

Fig. 1. Recovery of sperm crossovers. (**A**) Batches of sperm DNA from a hybrid mouse with heterozygosities (black and white circles) across the test region are amplified using two rounds of allele-specific PCR in repulsion phase (primers shown as black and white arrows) to selectively amplify recombinant molecules. Grey circles represent alleles of unknown status. (**B**) SNP typing is used to localize the breakpoint interval for each recombinant molecule amplified. (**C**) Examples of crossover molecules recovered at the E_β locus from $s \times k$ sperm DNA at 280 molecules per reaction, electrophoresed next to a 1 kb marker (Gibco) (M), and alongside 840 molecules per reaction of brain DNA.

Table I. Summary of sperm crossover data at the mouse MHC E_β gene for separate orientation A and B crossovers as well as for combined A + B exchanges

Cross	Orientation	No. sperm typed	No. crossovers recovered	Rate ($\times 10^{-3}$) (95% CI)	Centre (bp)[a]	Shift (bp)[b]	95% width (kb)[c]	Kolmogorov–Smirnov P[d]
$s \times b$	A	400 000	66	0.16 (0.13–0.21)	7070		0.7	
	B	240 000	63	0.26 (0.20–0.33)	7400	330	1.3	<0.001
	A + B	640 000	129	0.20	7190		1.0	
$s \times d$	A	120 000	79	0.66 (0.53–0.83)	7050		1.3	
	B	240 000	73	0.30 (0.24–0.38)	7350	300	0.8	<0.001
	A + B	360 000	152	0.42	7220		1.2	
$s \times k$	A	34 000	61	1.79 (1.40–2.35)	7190		0.9	
	B	44 000	63	1.43 (1.11–1.84)	7410	220	1.4	0.037
	A + B	78 000	124	1.59	7300		1.3	
$s \times p$	A	2 300 000	50	0.022 (0.016–0.028)	7050		0.9	
	B	3 100 000	61	0.020 (0.015–0.025)	7590	540	1.5	<0.001
	A + B	5 400 000	111	0.021	7280		1.6	
All four	A	2 900 000	256	–	7070		1.0	
	B	3 600 000	260	–	7470	400	1.2	<0.001
	A + B	6 500 000	516	–	7260		1.4	

[a]Based on position relative to DDBJ/EMBL/GenBank accession No. AF050157, clone BAC 135G15.
[b]Displacement of the centres of orientation B versus orientation A distributions.
[c]Width within which 95% of crossovers occur, assuming that they are normally distributed across the hotspot.
[d]Comparing orientation A and B crossover distributions.

methods). Mice homozygous for MHC haplotypes *b*, *d*, *k* or *p* were crossed with haplotype *s* homozygotes. Sperm DNA from a mature F_1 hybrid from each cross was prepared and E_β-recombinant DNA molecules recovered from multiple pools of sperm DNA by nested repulsion-phase allele-specific PCR directed to heterozygous single nucleotide polymorphism (SNP) sites, as shown in Figure 1. Nested PCR gave sufficient allele specificity to allow the selective amplification of crossover molecules even from large pools of sperm DNA (up to 30 000 amplifiable molecules of each progenitor haplotype per PCR). Parallel analysis of brain DNA yielded much lower levels of PCR products, establishing that the sperm crossovers recovered were genuine products of meiotic recombination (Jeffreys *et al.*, 2000) (Figure 1). Crossovers in reciprocal orientation were analysed either by using haplotype *s* 5′ allele-specific primers plus non-*s* 3′ primers (crossovers in orientation A) or 5′ non-*s* primers plus 3′ *s* haplotype primers (orientation B). We analysed a total of 6.5×10^6 amplifiable molecules from the four crosses and isolated 516 crossover molecules.

Sperm crossover rates in the E_β region varied significantly between different crosses (Fisher's exact test, $P < 0.001$ for each pair-wise comparison; Table I), but not between individuals from the same cross (data not shown). The $s \times k$ heterozygotes showed the highest crossover rate (1.6×10^{-3} per sperm) and $s \times p$ showing the lowest (0.021×10^{-3}). These rate differences were

Table II. List of ASO sequences

Marker name	Location (bp)[a]	ASO sequence				
		Haplotype *s*	Haplotype *b*	Haplotype *d*	Haplotype *k*	Haplotype *p*
0	4089	ccttggt**a**ccattaactg			ctttggt**g**ccattaactg	
0.04	4115	ctcactg**g**cccgagcaaa				ctcactg**a**cccgagcaaa
0.39	4453	taagagc**a**ctcttgggcc	taagagc**g**ctcttgggcc		taagagc**g**ctcttgggcc	
0.65	4723	tggcaat**c**gtcagggtga	tggcaat**g**gtcagggtga	tggcaat**g**gtcagggtga	tggcaat**g**gtcagggtga	
1.4-1	5480	ccagtctcc**g**ctgtcaat	ccagtctcc**a**ctgtcaat			
1.4-2	5482	ccagtctccgc**t**gtcaat		ccagtctccgc**a**gtcaat		
2.05	6114	tgtgttttttttt**a**ctg			tgtgttttttt**-**actg	
2.4	6472	ggtgcct**a**gatccacatg		ggtgcct**g**gatccacatg		ggtgcct**g**gatccacatg
2.45	6524	gctgtag**a**tgaagccaga		gctgtag**g**tgaagccaga		
2.64	6734, 6739	acccc**g**g**g**g**g**tg**g**gctgcc		acccg**a**ggg**a**ggctgcc		
2.7-1	6765	gcctgggg**g**tagtactgtgg	gcctggg**t**agtactgtgg		gcctggg**-**tagtactgtgg	
2.7-2	6768, 6775	gcctggggtag**t**actgtg**g**		gcctggggtag**a**actgtg**t**		gcctggggtag**a**actgtg**t**
2.82	6901	gtgtgtc**g**ggccctggag		gtgtgtc**a**ggccctggag		gtgtgtc**a**ggccctggag
2.85	6930, 6933	gggacc**g**aag**t**ggatttc		gggacc**a**aaa**a**tggatttc		
2.93	7016	gcttagct**c**acacttctt	gcttagct**t**acacttctt			
3.1	7158	tatagag**t**ccaggacaac	tatagag**c**ccaggacaac	tatagag**c**ccaggacaac	tatagag**c**ccaggacaac	tatagag**c**ccaggacaac
3.14	7206	gagtccccccccatcaat	gagtccc**tcccc**ccccca			
3.2	7247	cctaaag**g**cttacctaca				cctaaag**a**cttacctaca
3.3	7324	gtgtcag**a**tcaacataaa				gtgtcag**t**tcaacataaa
3.35	7393, 7399	gt**g**tggga**c**cacaacccc				gt**a**tggg**a**tcacaacccc
3.5	7575	gttatga**c**ttgttgccta				gttatga**t**ttgttgccta
3.58	7609	tggcctg**g**cttcttcagc		tggcctg**a**cttcttcagc		
4	8113	ggatcca**t**tctggatgga	ggatcca**g**tctggatgga	ggatcca**g**tctggatgga	ggatcca**g**tctggatgga	ggatcca**g**tctggatgga
4.48	8538, 8542	gaatgcc**c**gcc**c**gggtgg		gaatgcc**t**gcc**t**gggtgg		
4.58	8638	cttacag**t**gtaggtgcgt			cttacag**g**gtaggtgcgt	cttacag**g**gtaggtgcgt
4.8-1	8821, 8825	ggtcatg**a**ctga**a**ctcag	ggtcatg**g**ctga**c**ctcag			ggtcatg**g**ctga**c**ctcag
4.8-2	8823	tgac**t**gaactcagggaca		tgac**c**gac**c**tcagggaca		
5.4	9429	gccatggg**g**cactgccggt	gccatgg**t**cactgccggt			
5.79	9855	tgtaagg**a**gaggcctgaa			tgtaagg**t**gaggcctgaa	
5.9	9969	gaaggag**g**ttcccccccgg	gaaggaa**t**tcccccccgt			

Nucleotide differences are shown in bold.
[a]Based on position relative to DDBJ/EMBL/GenBank accession No. AF050157, clone BAC 135G15.

consistent both for orientation A crossovers and for orientation B exchanges (Table I), and are therefore reproducible. This establishes that recombination rates decrease in the order $k > d > b >> p$ in hybrids carrying haplotype *s*.

Allele-specific oligonucleotide mapping of crossover breakpoints

The selected polymorphisms (mainly SNPs) used to map crossover breakpoints by hybridizing amplified recombinant molecules with allele-specific oligonucleotides (ASOs) (Wood *et al.*, 1985) are shown in Table II. All 516 sperm crossovers were simple (Figure 1), with breakpoints mapping to a single inter-marker interval. There were no instances of more complex exchanges involving switching back and forth between haplotypes near the site of exchange. Crossover breakpoints were non-randomly distributed across the E_β region in all hybrids (Figure 2). Nearly all crossovers (99%) occurred within the second intron of the E_β gene and were highly concentrated in the 3′ half, demonstrating the presence of a highly localized hotspot. Crossover frequencies in each interval were used to determine the recombination activity per unit length in cM/Mb (Figure 2). Each hybrid showed an approximately normal distribution of combined orientation A + B crossover breakpoints across the hotspot (Figure 3A). All four heterozygotes showed the centre of the hotspot at a very similar location (Table I), within an MT element (Figure 2). The width of the hotspot was also similar in all crosses (1.0–1.6 kb), although the peak activity varied dramatically from 3.5 cM/Mb in the $s \times p$ hybrid to 170 cM/Mb in $s \times k$. The same hotspot therefore functions in male recombination in all heterozygotes, despite the substantial rate variation. Only one crossover, located upstream of position 6114 bp, was found outside the hotspot. The mean recombination activity over all crosses in DNA flanking the hotspot is therefore extremely low, at 0.005 cM/Mb (95% CI 0.0002–0.02 cM/Mb) and ~100-fold below the mouse genome average rate of 0.5 cM/Mb.

Reciprocal crossover asymmetry and transmission distortion

Orientation A and B crossovers were detected in each cross at similar frequencies, consistent with these sperm recombinants being the products of reciprocal crossover. Minor differences in A versus B rates within a cross (at most only 2.2-fold for $s \times d$; Table I) show no consistent bias towards A or B exchanges, and could easily have arisen from variation in PCR efficiency between different primer sets. While sperm crossovers appear to be reciprocal in rate, the separate A and B crossovers showed different distributions, with orientation A ($s \rightarrow$non-s) crossovers consistently displaced 5′-ward relative to orientation B (non-$s \rightarrow s$) exchanges in all four hybrids (Table I; Figures 2 and 3B). This displacement varied from 220 bp for $s \times k$ to 540 bp for $s \times p$, and averaged ~400 bp over all four heterozygotes.

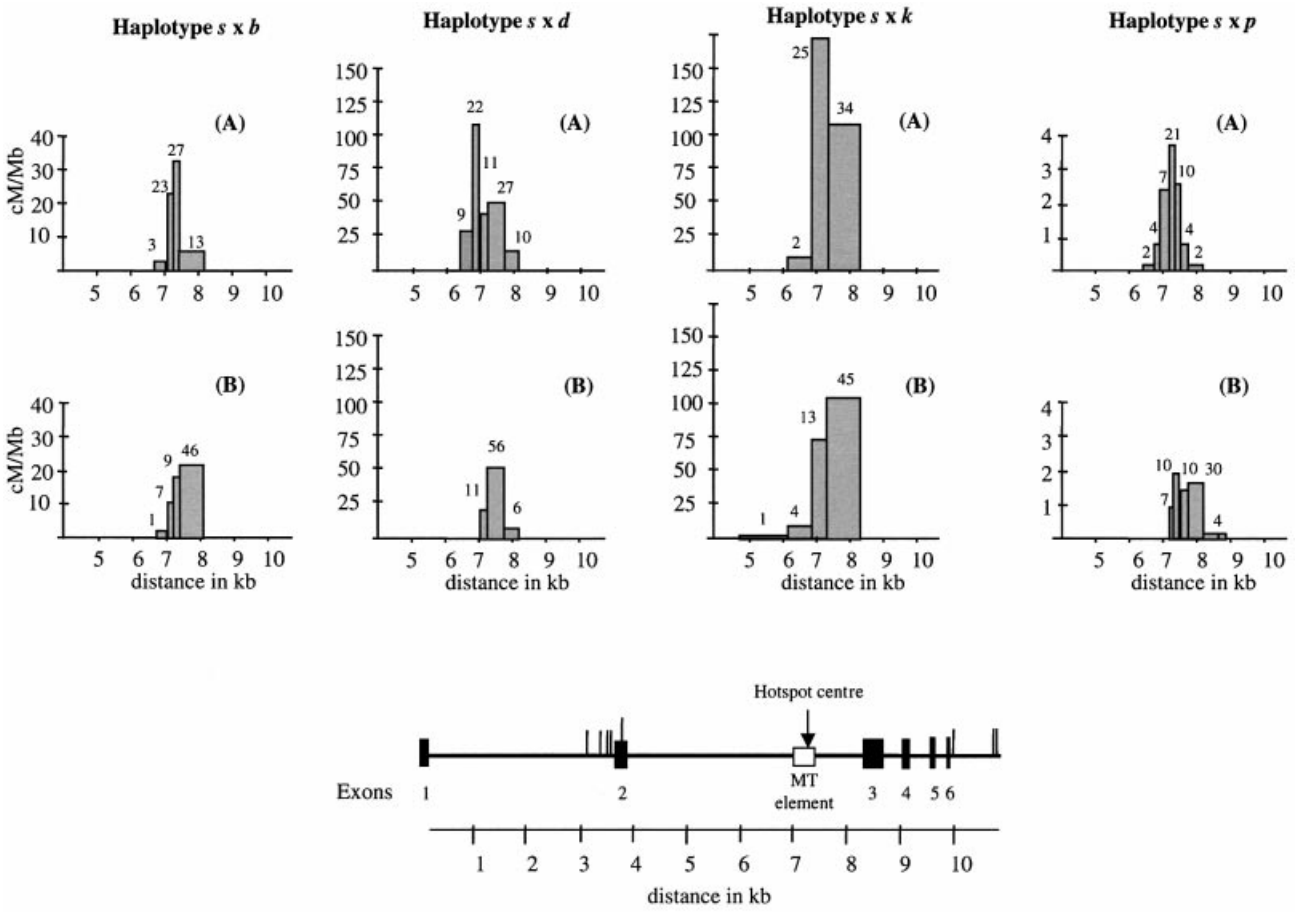

Fig. 2. Mouse E_β sperm crossover distributions for orientation A (*s*/non-*s*) and orientation B (non-*s*/*s*) recombinants. The haplotypes in each mouse analysed are given at top. The numbers of recombinants recovered in each interval, shown above the histograms, were used to calculate the crossover frequency per unit length of DNA for each interval in cM/Mb. Note the considerable differences in recombination scaling due to substantial variation in crossover activity across the hybrids tested. The E_β gene is shown beneath the histograms. The locations of the allele-specific primers used to recover crossovers are shown as vertical lines and the locations of the hotspot and MT element are indicated. Locations are relative to clone BAC 135G15 (DDBJ/EMBL/GenBank accession No. AF050157).

This reciprocal crossover asymmetry results in transmission ratio distortion of alleles into crossover products. Without asymmetry, *s* and non-*s* alleles should show a 50:50 Mendelian ratio in combined A and B crossovers. However, crossover asymmetry results in highly significant over-transmission of non-*s* alleles within the hotspot (Figure 4). The most extreme distortion was seen for marker 3.2 at 7247 bp, very close to the centre of the hotspot, which in $s \times p$ animals show a transmission ratio of 81:19 for non-*s*:*s* alleles in A + B crossover products. This distortion also affects neighbouring markers, with the strength of distortion decreasing with distance from the centre of the hotspot. Superimposition of data from all four hybrids (Figure 4, bottom) showed that the transmission distortion profiles were similar in all animals. However, the maximum degree of distortion varied between crosses in the order $p > (b, d) > k$; this order is the inverse of the order of crossover rates in these heterozygotes (Table I).

Discussion

Male recombination at the E_β hotspot

This work describes the application of high-resolution sperm typing to analyse meiotic recombination in the class II E_β gene in four mouse hybrid crosses. Our data confirm the presence of a recombination hotspot in the second intron of the gene, centred on an MT element and only 1.0–1.6 kb wide, and within the interval determined by prior mapping of recombinant inbred lines (Steinmetz *et al*., 1982, 1987; Bryda *et al*., 1992). This hotspot is flanked by DNA that is almost totally suppressed for recombination. Male crossovers are symmetrically distributed across the hotspot and occur at a rate strongly influenced by MHC haplotype. Sperm recombination rates for the $s \times b$, $s \times d$ and $s \times k$ crosses ($0.2–1.6 \times 10^{-3}$ per sperm) are comparable to crossover rates determined from pedigrees (1.0×10^{-3} across the E_β region; Passmore *et al*., 1987; Shiroishi *et al*., 1995), establishing that sperm analysis yields reliable quantitative data on male recombination.

Sequence determinants of recombination rates

It has previously been suggested that recombination rates across mouse MHC hotspots, as in other species, can be reduced by sequence divergence between the interacting haplotypes (Sant'Angelo *et al*., 1992; Yoshino *et al*., 1995). Datta *et al*. (1997) found that even a single mismatch over a 350 bp sequence between otherwise identical sequences in yeast can inhibit mitotic

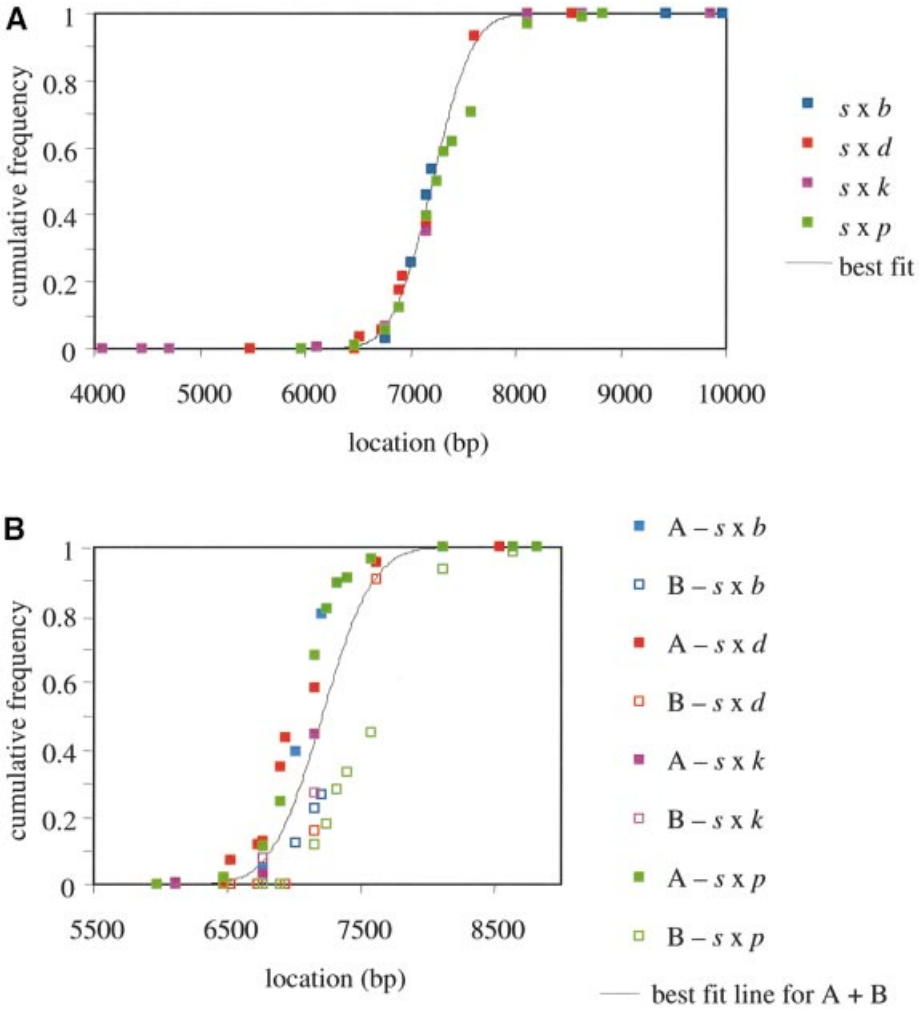

Fig. 3. Distribution of sperm crossovers across the E_β hotspot. (**A**) Cumulative frequency distributions of sperm crossovers in the four hybrids analysed, for the combined orientation A + B recombinants. The least-squares best-fit cumulative frequency distribution assumes that crossovers are normally distributed across the hotspot (centre at 7260 bp, standard deviation 350 bp). (**B**) Cumulative frequency distributions of separate orientation A (filled squares) and B (open squares) crossovers. The best-fit line for the combined A + B distributions is indicated. The B distributions are shifted 3′ relative to A distributions in all crosses.

recombination up to 4-fold; this anti-recombination was exerted through the action of mismatch repair proteins. Our data are consistent with the hypothesis that sequence divergence results in decreased recombination efficiency. The degree of divergence between the *s* haplotype and the other haplotypes over the central 200–400 bp of the hotspot is least for haplotype *k* (0.25%) and by far the greatest for haplotype *p* (2.5%) (Table III). The order of divergence from haplotype *s* over the centre of the hotspot ($k < d < b << p$) inversely correlates with the relative rates of recombination in the heterozygotes ($k > d > b >> p$), consistent with the hypothesis that recombination resulting in crossover is favoured when nucleotide identity is at its greatest at the E_β hotspot (Bryda *et al*., 1992; Sant'Angelo *et al*., 1992). However, it is possible that more distal flanking polymorphisms, as well as genetic background, could influence hotspot activity. For example, *cis*-acting elements have been shown to be involved in controlling recombination rates and sex-specificity at the mouse *Psmb9* hotspot (Shiroishi *et al*., 1991; Heine *et al*., 1994).

It has also been suggested that recombination may be influenced by an imperfect four-base repeat sequence $(AGGC)_n$ located just upstream of the third exon (8130 bp) and outside the hotspot (Kobori *et al*., 1986). This sequence shows similarity to the lambda phage chi sequence and 80% sequence identity to the human minisatellite core sequence (Jeffreys *et al*., 1985), and has been postulated to provide a recombination signal with the number of repeats governing the activity of the hotspot (Zimmerer and Passmore, 1991). Haplotype *s* has 11 copies of this repeat sequence, compared with 18 in haplotype *d*, 10 in *b* and *k*, and six in haplotype *p*. There is no obvious correlation between relative recombination rates (Table I) and either the absolute number of repeats or the difference in repeat copy number compared with haplotype *s*. There is therefore no clear evidence that this tetramer plays a role in regulating recombination activity.

Reciprocal crossover asymmetry and meiotic drive

Previous evidence of reciprocal crossover asymmetry between the *k* and *b* haplotypes at the E_β hotspot was based

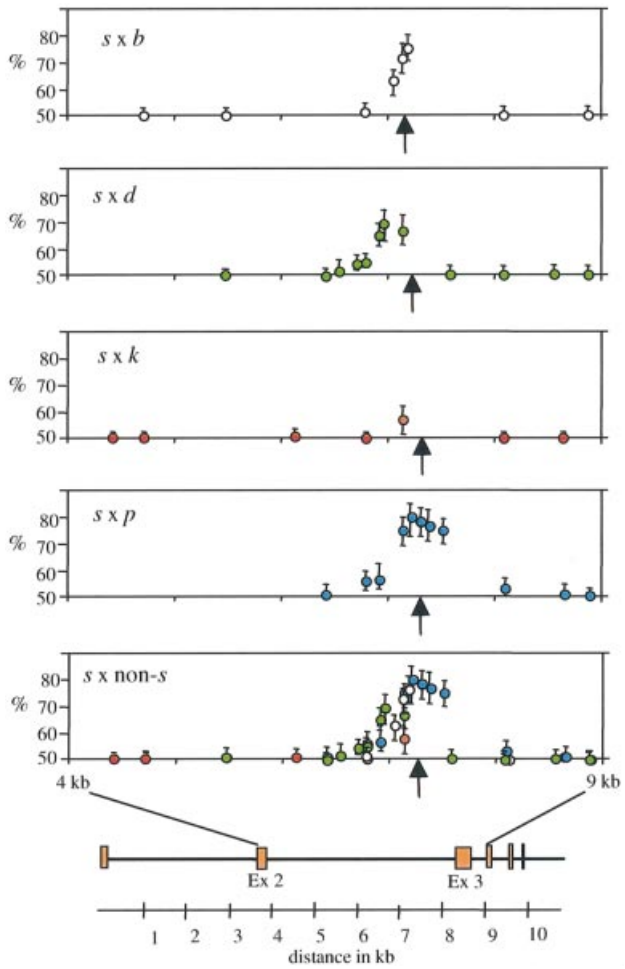

Fig. 4. Transmission distortion in E_β crossover products in each heterozygote. The proportions of non-*s* alleles in equal numbers of orientation A and B sperm crossovers are shown for each marker, along with 95% CIs. The bottom graph shows all hybrids superimposed. The positions of the markers with respect to the E_β gene are shown at bottom, and the centre of the hotspot is indicated with arrows.

on the mapping of only seven recombinants and was therefore very speculative (Zimmerer and Passmore, 1991). The large numbers of sperm crossovers analysed in the present study confirm that asymmetry in the location of reciprocal A and B crossover breakpoints does occur in all hybrids carrying haplotype *s*. It remains to be seen whether other heterozygous crosses will show a similar phenomenon. The asymmetry results in non-*s* alleles being preferentially over-transmitted to crossover products in all heterozygotes, with transmission distortion being strongest for markers closest to the centre of the hotspot (Figure 4). This phenomenon is remarkably similar to the asymmetry seen in one of the human MHC crossover hotspots (Jeffreys and Neumann, 2002). The degree of transmission distortion in human sperm crossover products (up to 87:13) is very similar to that seen in the E_β hotspot (up to 89:11), as is the degree of displacement of orientation A and B crossovers (on average 400 bp in E_β, compared with 430 bp in the human hotspot).

Reciprocal crossover asymmetry and transmission distortion can be readily explained by the double-strand break (DSB) repair model of recombination (Szostak *et al*., 1983; Pâques and Haber, 1999; Jeffreys and Neumann, 2002). This model is supported by previous data at human hotspots (Jeffreys *et al*., 2000, 2001; Jeffreys and Neumann, 2002) and at the *Psmb9* hotspot in mice (Guillon and De Massy, 2002) which show that crossovers are approximately symmetrical and normally distributed across a hotspot, compatible with the presence of initiation site(s) located at or close to the centre of the hotspot. Initiation creates a DSB, which then undergoes resection to create 3′ overhanging segments. The 3′ overhangs invade the undamaged chromosome where mismatch removal from the invading strand may occur (Alani *et al*., 1994), and repair is carried out using information from the undamaged (donor) chromosome (Jeffreys and Neumann, 2002). This process results in sites of crossover resolution occurring at distances from the initiation site determined, in part at least, by the extent of resection, and contributes to the observed width of hotspots.

If crossovers are initiated on both chromosomes with equal frequency, then breakpoints will be identically distributed in orientation A and B crossovers. However, if initiation rates vary between haplotypes, then asymmetry and transmission distortion will arise, increasing in strength with the degree of initiation suppression on one of the haplotypes (Jeffreys and Neumann, 2002). If a hybrid carries a high and low efficiency haplotype, then the majority of crossovers will arise from initiations on the active haplotype. DSB repair will therefore result in the replacement of markers from the initiating chromosome with those from the non-initiating donor chromosome, resulting in biased gene conversion in favour of the donor chromosome. The consistent over-transmission of non-*s* alleles in all heterozygous mice therefore suggests that haplotype *s* is most active in initiation. The relative strengths of transmission distortion in different crosses (Table I; Figure 4) further suggest that the initiation efficiency on different haplotypes decreases in the order $s > k > (b, d) > p$. The extreme over-transmission of the non-*s* allele (up to 89:11 in the $s \times p$ cross), combined with the inverse correlation between recombination rate and the strength of over-transmission, provides strong evidence in favour of this initiation model. Alternative models involving biased mismatch repair of heteroduplex DNA following strand invasion and subsequent branch migration are less plausible (for a fuller discussion see Jeffreys and Neumann, 2002).

There are, however, differences in the properties of reciprocal crossover asymmetry in the E_β hotspot and in the human MHC hotspot. In the latter, the trigger for asymmetry has been traced to a single SNP at the centre of the hotspot that, when heterozygous, appears to be

Table III. Number of sequence differences between haplotype *s* and each of the non-*s* haplotypes, around the centre of the E_β hotspot or over the whole second intron

Distance	Haplotype *b*	Haplotype *d*	Haplotype *k*	Haplotype *p*
±100 bp	2	1	0	4
±200 bp	3	2	1	10
Entire 2nd intron	12	86	8	Highly diverged[a]

[a]See section on haplotype *p* in the Discussion.

sufficient to cause asymmetry, presumably by directly influencing the efficiency of DSB formation (Jeffreys and Neumann, 2002). One SNP heterozygosity inside the E_β hotspot is shared by all four mouse hybrids (marker 3.1, located 100 bp 3′ of the average hotspot centre, with allele C shared by haplotypes *b*, *d*, *k* and *p*, and the alternative allele T on haplotype *s*), and the C allele is over-transmitted in every cross. However, without recombinant haplotype information, it is impossible to determine whether this SNP is triggering asymmetry. Given the variation in transmission distortion between different crosses, it is unlikely that this one SNP is exclusively responsible for asymmetry. Other hotspot SNPs might influence initiation in different heterozygotes, although this seems unlikely since first, they would always have to favour the *s* haplotype, and secondly, most SNPs within human MHC hotspots do not cause asymmetry (Jeffreys and Neumann, 2002). Instead, it seems likely that more distal elements influence the efficiency of recombination initiation in the E_β hotspot.

The second difference between the mouse and human hotspots is revealed by recombination rates. In the human hotspot, heterozygosity for the suppressing variant causes asymmetry but has little influence on crossover rate (in theory, the recombination rate in a heterozygote with one totally suppressed chromosome should be 50% of that in a person homozygous for the initiation-proficient variant) (Jeffreys and Neumann, 2002). In mice, recombination rates can be strongly suppressed in hybrids, particularly in $s \times p$ heterozygotes. This implies that in such hybrids, initiating events may be suppressed *in trans* on the *s* haplotype or, if they occur, fail to form a productive recombination complex. Perhaps sequence mismatches between haplotypes result in single strands from the *s* haplotype, produced by gap resection, that either fail to invade the other chromosome or are rejected on invasion. Subsequent DSB recombination repair may then occur preferentially from the sister chromatid, resulting in a sister chromatid exchange. Alternatively, mismatched invasions might be preferentially resolved to yield gene conversions rather than crossovers. The decrease of sperm crossover rates with increasing divergence from the *s* haplotype is consistent with these suggestions.

Exchanges involving haplotype p

Recombination has never before been detected between *p* and the other haplotypes at the E_β hotspot (Lafuse and David, 1986; Shiroishi *et al*., 1993). The present data indicate that this hotspot does function in $s \times p$ heterozygotes, but at a very low efficiency, apparently via recombination initiation occurring preferentially, if not exclusively, on the *s* haplotype. Yoshino *et al*. (1995) suggested that insertions and deletions (in their case at a tandem repeat locus at the *Psmb9* hotspot) may play a significant role in influencing recombination. In this respect, haplotype *p* is unique in containing a 597 bp ancestral DNA segment in the 5′ half of the second intron, outside the hotspot, that is replaced by a 1634 bp retroposon element in all other haplotypes (Zimmerer and Passmore, 1991). It is not clear how this insertion/deletion might influence E_β recombination. It has been suggested that this retroposon element creates a recombination initiation activator on non-*p* haplotypes (Zimmerer and Passmore, 1991). This would be very difficult to test, given that it would require analysis of *p*/non-*p* recombinant haplotypes either carrying or devoid of the retroposon.

Similarities between mammalian recombination hotspots

Several mammalian hotspots have been characterized using pedigree approaches, and more recently by high resolution sperm typing. The E_β hotspot shares remarkably similar features with human hotspots (Jeffreys *et al*., 1998, 2000, 2001), including the same width, the extreme suppression of recombination in the immediate flanking DNA, the simple structure of the vast majority of sperm crossovers and the evidence from crossover asymmetry for highly localized sites of initiation at the centres of hotspots. These shared features suggest that very similar recombination mechanisms operate in humans and in mice. Over-transmission of markers from recombination-suppressed haplotypes into crossover progeny also seems to be a common phenomenon in hotspots, having now been seen in one of six human MHC hotspots (Jeffreys and Neumann, 2002), in a human minisatellite-associated hotspot (Jeffreys *et al*., 1998) and in the mouse E_β hotspot. The resulting meiotic drive of markers from recombinationally suppressed chromosomes, which can include markers that actually suppress recombination, can be sufficiently strong to influence the population frequencies of alleles and to favour the eventual extinction of hotspot activity (Boulton *et al*., 1997; Jeffreys and Neumann, 2002). The prevalence and evolutionary significance of this recombination-based meiotic drive will require further high-resolution studies of meiotic crossover in a range of species.

Materials and methods

Mouse strains and breeding

Mice from strains A.SW, B10.S/SgmedJ (E_β haplotype *s*), C57BL/10J (E_β haplotype *b*), B10.D2 (E_β haplotype *d*), B10.A/SgSnJ (E_β haplotype *k*) and P/J (E_β haplotype *p*) were purchased from the Jackson Laboratory (Bar Harbor, ME) (haplotype and strain information available on the Jackson Laboratory website: www.jax.org). All relevant sequence information has been published previously (Saito *et al*., 1983; Widera and Flavell, 1984; Kobori *et al*., 1986; Padgett *et al*., 1991; Zimmerer and Passmore, 1991; Bryda *et al*., 1992). Mice with MHC haplotypes *b*, *d*, *k* and *p* were crossed with haplotype *s* mice. Caudal epidydimus and brains were collected from 8- to 10-week-old mature offspring. All crosses were generated at the University of Leicester under guidance issued by the MRC in 'Responsibility in the use of animals for medical research' and Home Office project license No. PPL 80/1353.

Genotyping and SNP verification

We used PCR primers designed from the sequenced clone BAC 135G15 (DDBJ/EMBL/GenBank accession No. AF050157) to identify and verify SNPs in the E_β gene of all strains in the study. We re-sequenced using BigDye Terminators (ABI) on an ABI 377 Automated Sequencer and identified SNPs using ABI AutoAssembler software. Selected SNPs were used to map recombination breakpoints in subsequent sperm analyses. The ASO probes used for genotyping are shown in Table II.

DNA extraction and quantification

Sperm DNA was prepared using procedures similar to those described by Jeffreys *et al*. (1994). To minimize the risk of contamination, all manipulations were carried out in a laminar flow hood. Caudal epidydimus from one mouse was chopped in 1 ml of phosphate-buffered saline (138 mM NaCl, 2.7 mM KCl, 5.4 mM Na_2HPO_4, 0.2 mM KH_2PO_4), filtered and centrifuged at 10 000 *g*. The cell pellet was resuspended in 1× SSC and somatic cells were lysed at room temperature

by the addition of SDS to 0.15%. The lysate was centrifuged and the resulting sperm pellet resuspended in 1 ml 0.2× SSC, 0.1% SDS, 1 M 2-mercaptoethanol and digested with 200 μg/ml proteinase K (Sigma) for 1 h at 37°C. DNA was recovered by phenol/chloroform extraction and ethanol precipitation. DNA from brain was prepared by tissue homogenization in 1× SSC, followed by SDS lysis, phenol/chloroform extraction and ethanol precipitation. All DNAs were dissolved in 5 mM Tris–HCl (pH 7.5). Approximately 20 μg of DNA was digested with enzymes (*Hpa*I, *Bss*HII or *Xho*I) that cleave outside the test interval analysed, to render genomic DNA fully soluble prior to dilution. DNA concentrations were determined by UV spectrometry and by agarose gel electrophoresis against λ phage DNA.

Sperm crossover analyses

We designed allele-specific primers 17–20 nt long with at least 50% GC content for SNP sites 5′ and 3′ of the putative E_β hotspot to amplify across a maximum of 7.7 kb. 5′ primers were located between 3227 and 4301 bp on the reference clone sequence, and 3′ primers between 9855 and 10952 bp. The 5′ allele-specific primers, named on the basis of distance from the first ASO typed (assigned as 0.0), were:
–1.0p, 5′-GGT GGG GAG GAT CTG AAA G-3′, used for haplotypes *d* and *p*;
–0.6g, 5′-TAA CTG TCC AGC CTG GGG-3′, used for haplotypes *b*, *d* and *k*;
–0.56A, 5′-TGC CCT GTT AGT TGT GGA-3′, used for haplotypes *b* and *k*;
–0.56T, 5′-TGC CCC GTT AGT TGT GGT-3′, used for haplotype *s*;
–0.57T, 5′-TTG GAG CTG GGG CAT GT-3′, used for haplotype *s*;
–0.5C, 5′-GGG TCT GGT CGG TCA TTC-3′, used for haplotype *s*;
–0.5T, 5′-CTT GGG TCT GGT CAT TT-3′, used for haplotype *p*;
–0.2C, 5′-GGA GCA AAA GCG GGC CGC-3′, used for haplotype *s*;
0.2F, 5′-CCT ACC TAC ACG GTG TGC GG-3′, used for haplotype *s*.
The 3′ primers were:
5.8T, 5′-CTG ACT GCT TCA GGC CTC T-3′, used for haplotype *s*;
5.8g, 5′-CTG ACT GCT TCA GGC CTC G-3′, used for haplotypes *p* and *d*;
6.75C, 5′-GGC CCA CAG CAA CAG CTT C-3′, used for haplotype *s*;
6.75T, 5′-GGC CCA CAG CAA CAT CTT T-3′, used for haplotypes *b* and *k*;
6.85C, 5′-CTC TTC CCA TCC TGC TGC-3′, used for haplotypes *b, d, k* and *p*;
6.85T, 5′-CTC TTC CCA TCC TGC TGT-3′, used for haplotype *s*.

The optimal annealing temperature for each primer was determined by amplification of inbred parental DNA samples from each strain, using the allele-specific primer in combination with an internal universal primer that can amplify from all haplotypes. Primers were selected that were both very efficient and highly specific for the allele of interest. Primers specific to the 5′ end of haplotype *s* were used in combination with primers specific to the 3′ end of the non-*s* haplotype to amplify orientation A crossovers, and vice versa for orientation B.

We amplified recombinant molecules using procedures similar to those described previously (Jeffreys *et al*., 2000, 2001). We amplified multiple batches of restriction-digested and diluted DNA samples, from sperm and brain of a single mouse per cross, each containing on average between 0.4 and 2 amplifiable crossover molecules per reaction. We tested two heterozygous mice for the *b* and *p* crosses, and one mouse each for the other two crosses. Since data for mice from the same cross were not significantly different (data not shown), such data were pooled. Brain DNA was used as a negative control for PCR artefacts and/or bleed-through amplification of one or other progenitor haplotype. DNA inputs depended on crossover rates and were determined in pilot experiments using 300–30 000 amplifiable molecules of each haplotype per reaction; we assume a single molecule PCR efficiency of 85% (Jeffreys *et al*., 2000). Poisson analysis of the number of positive and negative reactions (Jeffreys *et al*., 2000, 2001) was used to estimate the number of amplifiable crossover molecules. In the full crossover analyses, inputs varied from 216 ng sperm DNA per reaction (30 000 molecules) for $s \times p$ hybrids down to 2 ng DNA per reaction (280 molecules per reaction) for $s \times k$ crosses. DNA was amplified in two rounds of nested repulsion-phase PCR to selectively amplify recombinant molecules (Jeffreys *et al*., 1998, 2000) (Figure 1). Touch-down PCRs were used [typically 96°C for 1 min, followed by 26 rounds of 96°C for 20 s, 60–56°C for 30 s (step-down) and 63°C for 7–8 min (depending on length of amplicon)] with two allele-specific primers in repulsion phase. Primary PCR products were digested with S1 nuclease to remove single-stranded DNA and PCR artefacts (Jeffreys *et al*., 1998) and re-amplified with a second round of repulsion-phase allele-specific PCR as above. Secondary PCR products were electrophoresed on an agarose gel and visualized with ethidium bromide and UV light. Positive reactions were re-amplified using internal universal primers. PCR products were dot blotted and SNPs typed by ASO hybridization (Wood *et al*., 1985) as modified by Jeffreys *et al*. (2000) using the probes listed in Table II. Poisson estimations of the number of amplifiable recombinant molecules, to correct for instances of multiple recombinants recovered in a single positive reaction, were performed as described previously (Jeffreys *et al*., 1998).

Acknowledgements

We thank Dr John Stead, Dr Celia May, Liisa Kauppi and four anonymous reviewers for helpful comments, and Rita Neumann for help with ASO typing. This work was supported by grants to A.J.J. from the Royal Society and the Wellcome Trust (ref. 058084/Z/99/Z).

References

Alani,E., Reenan,R.A. and Kolodner,R.D. (1994) Interaction between mismatch repair and genetic recombination in *Saccharomyces cerevisiae*. *Genetics*, **137**, 19–39.

Boulton,A., Myers,R.S. and Redfield,R.J. (1997) The hotspot conversion paradox and the evolution of meiotic recombination. *Proc. Natl Acad. Sci. USA*, **94**, 8058–8063.

Bryda,E.C., DePari,J.A., Sant'Angelo,D.B., Murphy,D.B. and Passmore,H.C. (1992) Multiple sites of crossing over within the *Eb* recombinational hotspot in the mouse. *Mamm. Genome*, **2**, 123–129.

Datta,A., Hendrix,M., Lipsitch,M. and Jinks-Robertson,S. (1997) Dual roles for DNA sequence identity and the mismatch repair system in the regulation of mitotic crossing-over in yeast. *Proc. Natl Acad. Sci. USA*, **94**, 9757–9762.

Guillon,H. and de Massy,B. (2002) An initiation site for meiotic crossing-over and gene conversion in the mouse. *Nat. Genet.*, **32**, 296–299.

Heine,D., Khambata,S., Wydner,K.S. and Passmore,H.C. (1994) Analysis of recombinational hotspots associated with the p haplotype of the mouse MHC. *Genomics*, **23**, 168–177.

Jeffreys,A.J. and Neumann,R. (2002) Reciprocal crossover asymmetry and meiotic drive in a human recombination hotspot. *Nat. Genet.*, **31**, 267–271.

Jeffreys,A.J., Wilson,V. and Thein,S.L. (1985) Hypervariable 'minisatellite' regions in human DNA. *Nature*, **314**, 67–73.

Jeffreys,A.J., Tamaki,K., MacLeod,A., Monckton,D.G., Neil,D.L. and Armour,J.A.L. (1994) Complex gene conversion events in germline mutation at human minisatellites. *Nat. Genet.*, **6**, 136–145.

Jeffreys,A.J., Murray,J. and Neumann,R. (1998) High-resolution mapping of crossovers in human sperm defines a minisatellite-associated recombination hotspot. *Mol. Cell*, **2**, 267–273.

Jeffreys,A.J., Ritchie,A. and Neumann,R. (2000) High-resolution analysis of haplotype diversity and meiotic crossover in the human *TAP2* recombination hotspot. *Hum. Mol. Genet.*, **9**, 725–733.

Jeffreys,A.J., Kauppi,L. and Neumann,R. (2001) Intensely punctate meiotic recombination in the class II region of the major histocompatibility complex. *Nat. Genet.*, **29**, 217–222.

Khambata,S., Mody,J., Modzelewski,A., Heine,D. and Passmore,H.C. (1996) Ea recombinational hotspot in the mouse major histocompatibility complex maps to the fourth intron of the *Ea* gene. *Genome Res.*, **6**, 195–201.

Kobori,J.A., Strauss,E., Minard,K. and Hood,L. (1986) Molecular analysis of the hotspot of recombination in the murine major histocompatibility complex. *Science*, **234**, 173–179.

Lafuse,W.P. and David,C.S. (1986) Recombination hotspots within the I region of the mouse H-2 complex map to the E_β and E_α genes. *Immunogenetics*, **24**, 352–360.

Lafuse,W.P., Lee,S.T., Castle,L. and David,C.S. (1989) Restriction fragment analysis of H-2 recombinant mouse strains with crossovers between *Eα* and *C4* genes. *Immunogenetics*, **30**, 387–389.

Padgett,K.A., Shreffler,D.C. and Saha,B.K. (1991) Molecular mapping of murine I region recombinants. III. Crossing over at two discrete sites within the beta 1–beta 2 intron of the E beta gene. *J. Immunol.*, **147**, 2764–2770.

Pâques,F. and Haber,J.E. (1999) Multiple pathways of recombination induced by double-strand breaks in *Saccharomyces cerevisiae*. *Microbiol. Mol. Biol. Rev.*, **63**, 349–404.

Passmore,H.C., Kobori,J.A., Zimmerer,E.J., Spinella,D.G. and Hood,L. (1987) Molecular characterization of meiotic recombination within the major histocompatibility complex of the mouse: mapping of crossover sites within the I region. *Biochem. Genet.*, **25**, 513–526.

Petes,T.D. (2001) Meiotic recombination hotspots and cold spots. *Nat. Rev. Genet.*, **2**, 360–369.

Pittman,D.L. and Schimenti,J.C. (1998) Recombination in the mammalian germ line. *Curr. Top. Dev. Biol.*, **37**, 1–35.

Saito,H., Maki,R.A., Clayton,L.K. and Tonegawa,S. (1983) Complete primary structures of the E_β chain and gene of the mouse major histocompatibility complex. *Proc. Natl Acad. Sci. USA*, **80**, 5520–5524.

Sant'Angelo,D.B., Lafuse,W.P. and Passmore,H.C. (1992) Evidence that nucleotide sequence identity is a requirement for meiotic crossing over within the mouse Eb recombinational hotspot. *Genomics*, **13**, 1334–1336.

Shiroishi,T., Sagai,T., Hanzawa,N., Gotoh,H. and Moriwaka,K. (1991) Genetic control of sex-dependent meiotic recombination in the major histocompatibility complex of the mouse. *EMBO J.*, **10**, 681–686.

Shiroishi,T., Sagai,T. and Moriwaki,K. (1993) Hotspots of meiotic recombination in the mouse major histocompatibility complex. *Genetica*, **88**, 187–196.

Shiroishi,T., Koide,T., Yoshino,M., Sagai,T. and Moriwaki,K. (1995) Hotspots of homologous recombination in mouse meiosis. *Adv. Biophys.*, **31**, 119–132.

Steinmetz,M., Minard,K., Horvath,S., McNicholas,J., Srelinger,J., Wake,C., Long,E., Mach,B. and Hood,L. (1982) A molecular map of the immune response region from the major histocompatibility complex of the mouse. *Nature*, **300**, 35–42.

Steinmetz,M., Uematsu,Y. and Fischer Lindahl,K. (1987) Hotspots of homologous recombination in mammalian genomes. *Trends Genet.*, **3**, 7–10.

Szostak,J.W., Orr-Weaver,T.L., Tothstein,R.J. and Stahl,F.W. (1983) The double-strand-break repair model for recombination. *Cell*, **33**, 25–35.

Widera,G. and Flavell,R.A. (1984) The nucleotide sequence of the murine I–E β b immune response gene: evidence for gene conversion events in class II genes of the major histocompatibility complex. *EMBO J.*, **3**, 1221–1225.

Wood,W.I., Gitschier,J., Lasky,L.A. and Lawn,R.M. (1985) Base composition-independent hybridization in tetramethyleammonium chloride: a method for oligonucleotide screening of highly complex gene libraries. *Proc. Natl Acad. Sci. USA*, **82**, 1585–1588.

Yoshino,M., Sagai,T., Fischer Lindahl,K., Toyoda,Y., Moriwaki,K. and Shiroishi,T. (1995) Allele-dependent recombination frequency: homology requirement in meiotic recombination at the hotspot in the mouse major histocompatibility complex. *Genomics*, **27**, 298–305.

Yu,A. *et al*. (2001) Comparisons of human genetic and sequence-based physical maps. *Nature*, **409**, 951–953.

Zimmerer,E.J. and Passmore,H.C. (1991) Structural and genetic properties of the Eb recombinational hotspot in the mouse. *Immunogenetics*, **33**, 132–140.

Received July 10, 2002; revised January 20, 2003; accepted January 27, 2003